Available online at www.sciencedirect.com
SCIENCE DIRECT®
Carbohydrate Research 339 (2004) 2701–2711
Carbohydrate RESEARCH

Flexible chitin films: structural studies

Nealda Leila Binte Muhammad Yusof,[c] Lee Yong Lim[b] and Eugene Khor[a,*]

[a]*Department of Chemistry, National University of Singapore, 3 Science Drive 3, Singapore 117543, Singapore*
[b]*Department of Pharmacy, National University of Singapore, 18 Science Drive 4, Singapore 117543, Singapore*
[c]*Biomedical Research and Support Services P.L., 59 Ubi Avenue 1, #06-04 Bizlink Center, Singapore 408938, Singapore*

Received 15 June 2004; accepted 3 September 2004
Available online 12 October 2004

Abstract—Chitin gels were transformed into thin, flexible chitin films with minimal dimensional shrinkage and maximum flexibility and thickness in the range of 25–80 μm by a cold-press process. Solvent residue was removed by heating the films at 50 °C for 12 h, followed by rinsing in 95% ethanol. The crystallinity and mechanical properties of the flexible chitin films were found to be a function of the amount of shrinkage from the gel to the final film that was obtained. For 28-μm thick films with 30% shrinkage, transparency of up to 90% was found. X-ray diffractometry (XRD) showed that the number of diffraction peaks appearing at $2\theta = 23°$ and $2\theta = 27°$ became increasingly sharper with shrinkage. Topographical information obtained from scanning electron microscopy (SEM) and atomic force microscopy (AFM) attributed the structural morphology of the films to the formation of sub-microscopic micelles. Scanning transmission electron microscopy (STEM) showed that shrinkage resulted in coarser microstructure, affecting tensile properties, where the ductility and toughness were proportional to the amount of shrinkage. These flexible chitin films have potential as wound dressing materials.

Keywords: Chitin film; Flexible; Transparent; Shrinkage; Tensile properties

1. Introduction

Chitin's most abundant crystalline form, α-chitin, is highly ordered with extensive hydrogen bonding between adjacent polymer chains of the predominantly β-(1→4)-linked 2-acetamido-2-deoxy-D-glucose. This makes chitin a rigid and intractable material exhibiting poor solubility, swellability, reactivity, and processability. Despite these drawbacks, chitin continues to receive widespread attention because of its abundance, biodegradability, nontoxicity, chemical inertness, and its many potential industrial applications.

Research to convert chitin into forms that are practical, efficient, and user-friendly over the past 30 years has grudgingly yielded gels, films, fibers, and sponges.[1–4] Among the strategies that have been invoked is the use of chemical derivatization to overcome the rigidity of chitin. Many chitin derivatives can be readily cast into films, be incorporated with plasticizers to impart flexibility to the films, processed into wet-mat fibers and subject to polymer cold-drawing processes.[5–12] The drawback of chemical modification, adding of plasticizers and wet-mat and cold-drawing processes are that they incur the use of extra reagents, create extra steps in the production cycle, and may introduce toxic residues into the final product. Therefore, a need still exists to process chitin into useful materials via fast and cost-effective processes that preserve its original character.

The primary cause for the brittleness and dimensional distortion of dry chitin materials formed from its solution is the coalescence of chitin chains on contact with moisture leading to coagulation and shrinkage as hydrogen bonds between adjacent chitin chains form. Therefore, the challenge is to 'manage' the coagulation and shrinkage process during the preparation of chitin materials so that they retain flexibility, reduced dimension distortion, and superior mechanical integrity in the dry

* Corresponding author. Tel.: +65 6874 2836; fax: +65 6779 1691; e-mail: chmkhore@nus.edu.sg

0008-6215/$ - see front matter © 2004 Elsevier Ltd. All rights reserved.
doi:10.1016/j.carres.2004.09.008

state. Our interest in preparing flexible chitin film for biomedical and membrane applications led us to develop a strategy specifically to 'manage' the formation of these inter- and intra-molecular hydrogen bonds between adjacent chitin chains that affect the final crystalline structure in the solid state. We report the successful preparation of chitin films that are flexible and transparent, with minimum shrinkage and distortion, and explain the causes of rigidity in chitin and its management by studying the changes that occur during the making of thin chitin films with X-ray diffraction, microscopy and mechanical characterization techniques.

2. Materials and methods

2.1. Chemicals and reagents

Chitin was obtained from Polysciences, Inc. and purified prior to use at room temperature using an in-house protocol of treating with 5% NaOH solution for 7 days, after which the chitin was rinsed with water until pH neutral. Subsequently the chitin was treated with 1 M HCl for 1 h, washed till pH neutral, and dried. *N*,*N*-Dimethylacetamide (DMAc) was of analytical grade. Technical grade 95% ethanol was distilled prior to use. Deionized water was obtained by passing tap water through a Micromeg M&S ion mixed-bed exchanger.

2.2. Film preparation

Chitin flakes were dissolved in DMAc–5% LiCl at 10 °C to give a 0.5% chitin solution that was filtered through glass wool. The chitin solution (155 mL) was cast into a deep mold with base dimensions of 15×25 cm. The solution height in the mold was maintained at 1 cm. The molds were covered with aluminum foil. Pinholes were made on the foil with a needle to permit interaction with atmospheric moisture (relative humidity 80–100%) at room temperature (25–27 °C) in a fume hood to give chitin gels. Gelling times were set at ~24 and ~96 h to achieve minimum and maximum gel shrinkages, respectively.

Films P24 and P96 were derived by a cold-press method. Essentially the chitin gel was placed between two sheets of filter paper, one on either side. Two glass plates were next placed, one on either side of the filter paper, to form a 'sandwich' where the chitin gel was in the middle. The glass plates were held together by paper clamps at room temperature. The clamps effectively pressed the gel until the gel's thickness was reduced. The gel assembly was next heated at 50 °C in an oven for 12 h to remove residual solvent. Films P24 and P96 were subsequently soaked in 95% ethanol, and the cold-press procedure was repeated and maintained for 48 h to give dry, DMAc-free, flexible chitin films. The ethanol effluent was tested by HPLC to ascertain it was DMAc free. Film P24W was derived from chitin gels that were first rinsed in water after 24 h of coagulation, followed by press drying to give thicker films. Film 24W was obtained after rinsing the gels in water after 24 h of coagulation and air-drying without pressing. All chitin films were stored at room temperature and 30% relative humidity. Table 1 summarizes the production of each film type.

Table 1. Production of chitin films

Film	Method	Transparency (visual observation)	Color
P24	Gel for 24 h Cold-press Ethanol wash Cold-press and dry	Transparent	Colorless
P96	Gel for 96 h Cold-press Ethanol wash Cold-press and dry	Transparent	Light yellow
P24W	Gel for 24 h Water wash Cold-press and dry	Translucent	Light yellow
W24	Gel for 24 h Water wash Dry	Opaque	Yellow

2.3. Film characterization

The transparency of each film was obtained by measuring its transmittance with a Shimadzu UV-1601 UV–vis spectrophotometer between 400 and 800 nm using air as reference. The crystallographic orientation and the relative amount of crystallinity in each film were measured using a Siemens D5005 X-ray diffractometer (XRD) operated at 40 kV, 40 mA, between $2\theta = 5°$ and $2\theta = 70°$. Diffractograms were measured by the reflection method with copper-filtered Cu Kα radiation source. Topographical imaging of the sample surfaces was obtained with an AFM (Nanoscope® IIIa Dimension 3000) in the Tapping mode™. A scan size of 3 μm was used to give a magnification of approximately 51,600×. Images were obtained with an etched silicon tip attached to a cantilever of a length of 125 μm, a width of 30–40 μm, a tip height of 10–15 μm, a force constant of 20–100 N/m and a resonant frequency of 200–400 Hz. The mechanical behavior of film samples were obtained with an INSTRON 4302 uniaxial tensile tester using a 1 kN load cell at 26 °C, relative humidity of 50% and a crosshead speed of 1 mm/min. The test dimensions of samples conformed to ASTM D882 recommendations. Cleavage morphology of the chitin films fractured in liquid nitrogen was obtained by scanning transmission electron microscope (STEM) with a JEOL JEM-100CX II electron microscope, at 8000×

magnification and 40 kV filament voltage. Film surface morphology was obtained by scanning electron microscopy (SEM) with a JEOL JSM-T220A, at 100× magnification and 15 kV filament voltage. Samples for electron microscopy were gold coated by ion sputtering (JEOL JFC-1100) for 4 min.

3. Results and discussion

3.1. Preparation of chitin films

Hitherto, chitin films have typically been prepared by solution casting methods where solvent removal leads to a gel state that is subsequently dried to give chitin films.[13,14] In all instances, considerable dimensional shrinkage, hardening, and brittleness is found in the final chitin film, attributed to the nonuniform drying and reorganization of the chitin polymer chains to form highly crystalline α-chitin in the solid state. Therefore, an improved method to make chitin films with both strength and conformability would be useful for film applications of chitin. A cold-press step has been found to impart the properties of flexibility, conformability, and strength to chitin films coagulated from its solution. The cold-press step is essentially a method of applying uniform mechanical pressure at room temperature, to control the inherent shrinkage of chitin as it transforms from a solution, through a gel and finally, solidifying to give chitin films that in the process 'arrests' the reorganization of the chitin structure.

Cold-pressing is the chitin analog to ceramic powder pressing where a powdered mass, usually containing a small amount of water and binder, is compacted into the desired shape by pressure.[15] In the chitin context, cold-pressing is used to impede the mobility, coalescence, and packing of chitin polymer chains during solvent removal, resulting in reduced shrinkage and limiting the extensive inter- and intra-chain hydrogen bonding. Cold-pressing also reduces the thickness of chitin films that give rise to specific structural morphologies, imparted transparency, and formed structurally less packed chitin in the solid state.

3.2. General film characteristics

The cold-press method has been found to influence the final characteristics of the chitin film when applied at specific gelling stages. The observed film characteristics based on cold-press methodology can be explained as follows. The chitin solution obtained after 24 h of coagulation gave a chitin gel that was the softest and most flexible, yet fragile because of the limited extent of consolidation of chitin chains and care was exercised in handling the gel. The chitin gel was immediately cold-pressed after 24 h of coagulation to give film P24 with minimum shrinkage, shape and dimension retention, transparency, softness, conformability, and flexibility of the original chitin gel precursor. As gel time increased from 24 to 96 h, the chitin gel that formed pulled away from the sides of the mold with a corresponding decrease in size. This is because prolonged exposure to environmental water vapor further insolubilized the chitin through the coalescence of chitin chains resulting in shrinkage. The simultaneous expulsion of solvent leads to the tightening of the gel structure as chitin chains pack closer, giving a stiffer chitin gel. The immediate cold-pressing of the chitin gel coagulated for 96 h gave film P96 that was still found to be transparent, retained its shape but was less flexible, as indicated by the harder and stiffer nature of the precursor chitin gel.

To obtain a contrast effect of the shrinking on the final film character, a chitin gel obtained after 24 h coagulation was submerged in water prior to cold-press treatment. The strong nonsolvent effects of water caused rapid coagulation and drastic shrinking of the chitin gel, aided by the aggregation of chitin chains as they reconstitute into the strong inter- and intra-chain hydrogen bonds. Subsequent cold-press after the water treatment produced film P24W that was translucent and stiffer than film P96 with considerable shrinkage from the original dimensions of the precursor chitin gel. The exclusion of cold-press after the water treatment produced film 24W, essentially the de facto method of making chitin films where the gel is left to air dry on its own to give a dry, sometimes curled film that exhibited the most shrinkage, deformation, rigidity, opacity, and brittleness.

Figure 1 relates the total percent shrinkage area of the chitin films to their thickness and transparency (Fig. 1a–c). As the shrinkage increased, the surface area decreased accordingly with a corresponding increase in thickness, a clear indication of chitin chain consolidation. The order of transparency of the chitin films was found to be P24 P96 > P24W > 24W. Decreasing transparency was a function of increasing material density, a result of shrinkage and chitin chain packing and is an inverse relationship between the observed transparency and the total shrinkage area.

The difference in transparency between films P96 and P24W with comparable shrinkage values was attributed to P24W having a more extensive material consolidation and chain packing from the interaction with water, imposing strong nonsolvent effects, that occurs prior to cold-pressing. Shrinkage-activated packing is less drastic in film P96 as cold-pressing effectively 'froze-in' the characteristics of the precursor chitin gel, arresting chitin chain rearrangement that led to a lack of packing density in some regions, giving a less organized structure in the dried film, enhancing transparency.

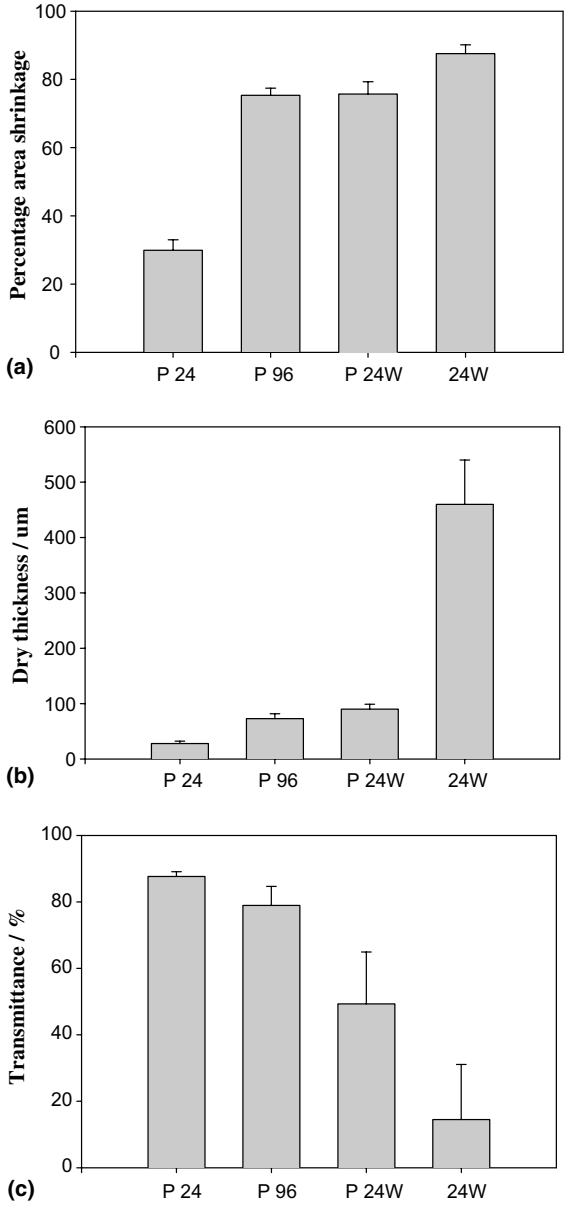

Figure 1. Physical measurements and transparency of chitin films: (a) percentage area shrinkage, (b) dry thickness, (c) percentage transmittance of chitin film samples.

3.3. Prediction of the degree of packing by X-ray diffraction (XRD) analysis

Figure 2 shows the X-ray diffractograms for the chitin films P24, P96, P24W, and 24W, displaying the characteristic crystalline peaks of chitin at $2\theta = 9.421°$ (peak I) and 19.563° (peak II) due to the presence of (0 2 0) and the mixture (1 1 0) and (0 4 0), respectively. Three additional peaks (III, IV, and V) between $2\theta = 22°$ and 45°, attributed to orientation (1 0 1) at $2\theta = 22.5°$, (1 3 0) at $2\theta = 24°$ and (0 1 3) at $2\theta = 26°$, were also obtained. These five peaks are in agreement with the XRD findings of Seong et al. reported for chitin.[16–18] However, an additional signal not reported by Seong et al. at $2\theta = 39°$ (Peak VI) was also found.

The intensity of peaks III, IV, and V vary with film type. Peaks III and IV were least pronounced for film P24, but became progressively sharper for films P96, P24W, and 24W. Peak V was, however, more pronounced for P24, increasingly broadening from P96 to P24W and 24W. This was attributed to the emergence of peak IV causing peak V to merge with the former to form an almost indiscernible signal. The number of X-ray peaks increased in the order of P24, P96, P24W, and 24W. There were four peaks assigned to P24 (I, II, V, and VI). A shoulder (peak III) to the right of peak II appeared for P96. All six peaks (I, II, III, IV, V, VI) appeared for both films P24W and 24W. Peak VI was the most distinct for films P24W and 24W.

The full-width-at-half-maximum (FWHM) value of the major peak II decreased significantly and progressively from P24, P96, and P24W to 24W due to the emergence of the shoulder, peak III. The additional X-ray peaks observed for P96, P24W, and 24W and the sharpening of peak II for these films probably indicate that crystalline orientation becomes increasingly established with shrinkage. Certain crystalline domains were, therefore, absent or seen as broader peaks in P24, due to the lack of shrinkage and the opportunity for extensive chain packing in this film.

XRD data showed that the chitin films could be made to assume slightly different solid-state crystalline struc-

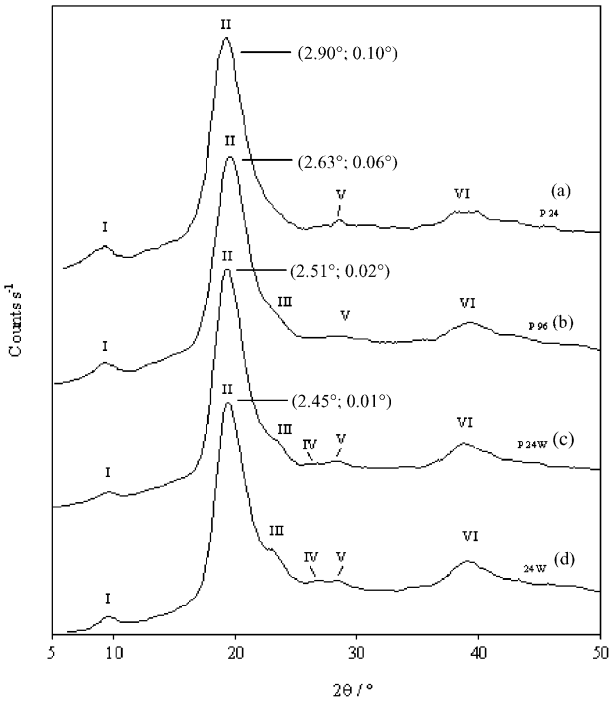

Figure 2. X-ray diffractograms of chitin films: (a) P24, (b) P96, (c) P24W, (d) 24W. Figures in parentheses = FWHM (average; standard deviation).

tures by the cold-press of chitin gels of various gelling durations. Film 24W served as the reference material since it was formed using the de facto method, and its crystal structure has been fully established. Films P24W and 24W were both formed by washing coagulated chitin gels in water. Their crystal diffractograms were similar, although film P24W was later pressed until dry. Films P24 and P96 were formed by pressing freshly coagulated chitin gels prior to any wash treatments. The (1 0 1) and (1 3 0) orientations were either absent or weak in their diffractograms, indicating a less established crystalline structure. This slight difference in crystalline structure influenced the chitin film characteristics significantly. Films P24 and P96 were considerably softer, thinner, more flexible and conformable than film P24W. Film P24, especially, had a flexible, soft texture similar to high-density polyethylene (HDPE) films commonly used as packaging material. Film P96, having shrunk much more, was slightly stiffer than film P24. Film 24W was brittle and tended to crack easily on bending. Therefore, X-ray results supported the qualitative physical observations.

3.4. Observation of material packing by scanning transmission electron microscopy (STEM) and atomic force microscopy (AFM)

Figure 3 shows the STEM images of film cleavage surfaces at 8000× magnification. Films P24 and P96 displayed relatively smooth and uniform cleavage surfaces. The cleavage topography of film P24W was rough, heavily dimpled, and extremely fibrous. Larger and more angular features ran longitudinally along the cleavage surface of film 24W. All the films P24, P96, P24W, and 24W showed a characteristic longitudinal alignment of features on their cleavage surfaces (arrow), indicative of the parallel orientation of chitin. Blackwell et al. proposed that the parallel chitin chains were arranged in bonded 'piles' or 'sheets' linked by N–H···O=C hydrogen bonds through the amide groups (Fig. 4b). The O–H group attached to the C-6 carbon atom of the hydroxymethyl side chain was also hydrogen bonded to the oxygen of a similar group from a neighboring chain running in the opposite direction (Fig. 4c).[19]

FTIR results support that chitin–chitin hydrogen bonding increased with film shrinkage from films P24, P96, P24W, and 24W. Figure 5 show a broadening of the out-of-plane O–H deformation band shifting to higher frequencies as hydrogen bonding increased from $610\,cm^{-1}$ for P24, $641\,cm^{-1}$ for P96 to $648\,cm^{-1}$ for P24W. The out-of-plane O–H deformation band broadened significantly for film P24W to overlap with the $898\,cm^{-1}$ cyclic band that was otherwise seen in the spectra of films P24 and P96, a direct result of an increased *p* character in the lengthened O–H bonding in chitin, making it easier to stretch but more difficult to bend. The relatively higher out-of-plane bending frequency for P24W was attributed to the stronger chitin–chitin hydrogen bonds in a highly packed structure. That is to say, the

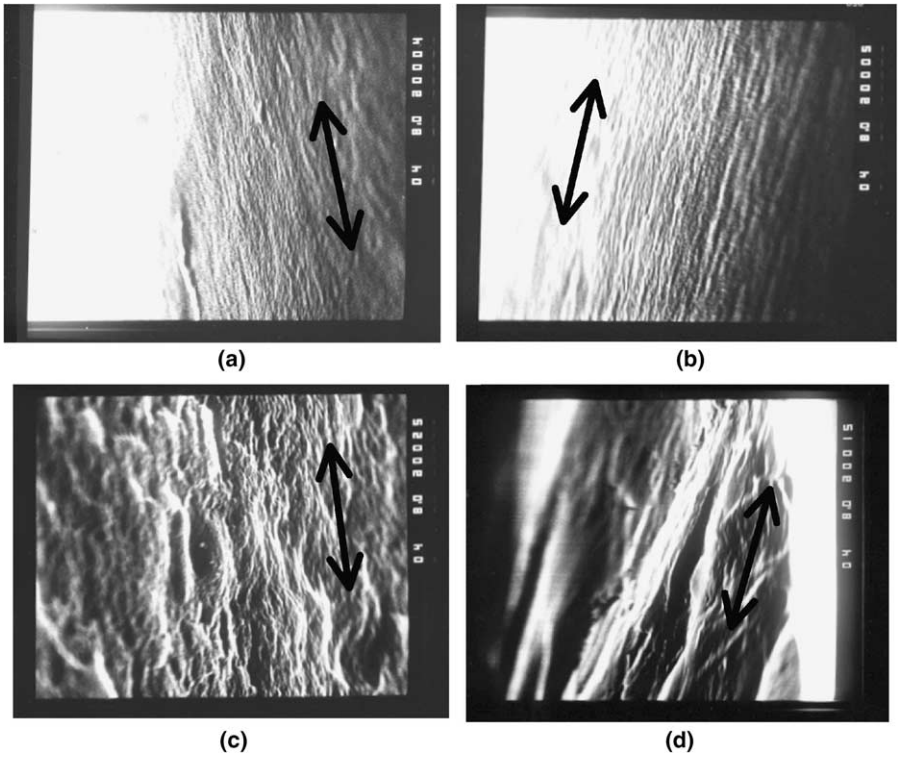

Figure 3. Cleavage surface of chitin films: (a) P24, (b) P96, (c) P24W, (d) 24W.

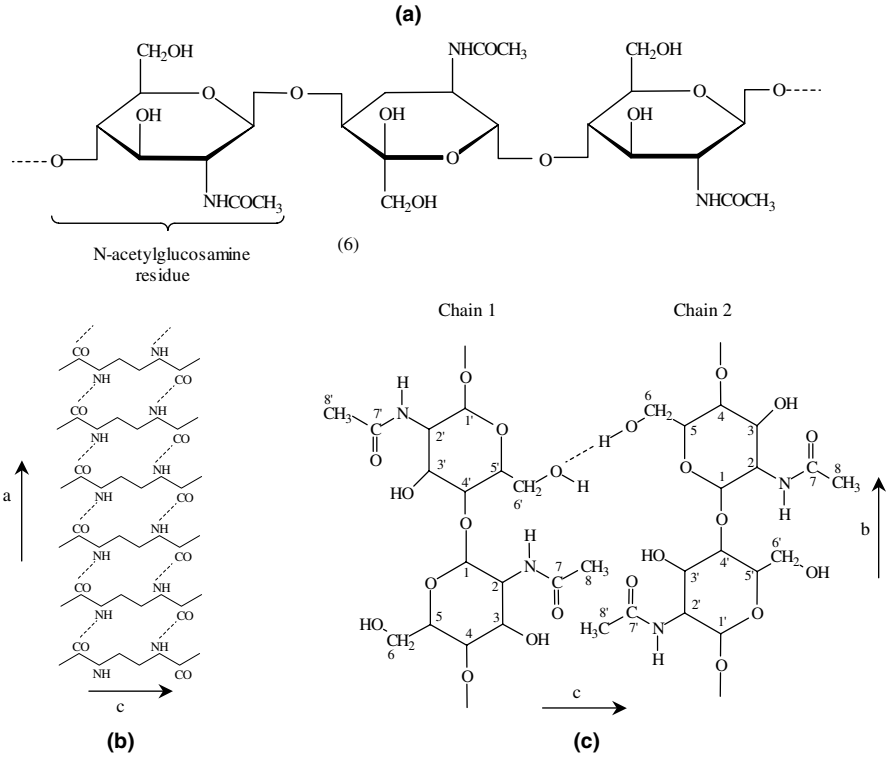

Figure 4. Schematic of the hydrogen-bonding interactions present in chitin: (a) structure of chitin, (b) pile or sheet of chitin chains along the fiber axis; hydrogen-bond direction, a, and side-chain direction, c (Ref. 18), (c) inter-chain hydrogen bonding between hydroxymethyl groups on a plane perpendicular to the fiber axis.

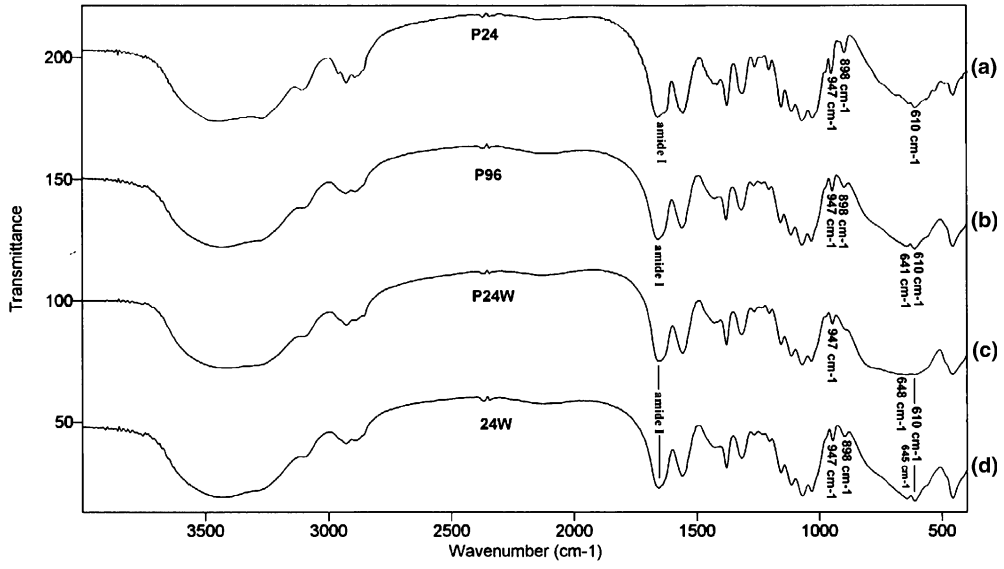

Figure 5. FTIR spectra showing shifts in the amide I stretching and the O–H deformation bands for chitin films: (a) P24, (b) P96, (c) P24W, and (d) 24W.

total *p* frequency shift can mostly be ascribed to the extensive hydrogen-bond interactions between chitin chains in film P24W compared to the weaker chitin–solvent hydrogen bonds that act to stabilize the structure of films P24 and P96. There was also a slight shift of the amide I band to lower wavenumbers from 1660 cm^{-1} for P24 and 1658 cm^{-1} for P96, to 1656 cm^{-1} for P24W, characteristic of increased hydrogen bonding. For film 24W, both the O–H deformation and amide I bands were found at frequencies similar to those of film

P96, but lower than those of film P24W, despite having undergone the largest shrinkage.

Figure 6 shows the 2D and 3D AFM images of the top surface of all film types. Generally, the 2D image of film P24 showed a scatter of small surface features seen as bright dots. The corresponding 3D image of film P24 displayed small spikes with some regions of coalescence (arrow). Going from films P96 and P24W to 24W, there was a gradual clustering of the finer surface features found in P24 progressively coalescing into big mounds that was in line with increased shrinkage in the 2D images. This was more pronounced in the corresponding 3D images where the small spikes began to coalesce in P96, leading to ridge-like features in P24W and finally large mounds in 24W.

The AFM observations of chitin could be attributable to the sub-microscopic micelle structure resulting from hydrogen bonds between the aminoacetyl groups in the chitin molecules.[13,20] Austin and Brine described chitin as having a high degree of spherulitic crystallinity under a polarizing microscope.[21] The uniformly distributed small surface features of film P24 suggests that the coagulation of chitin arising from the interaction of chitin chains form well-spaced sub-microscopic micellar islands. This results in a homogeneous, almost featureless and relatively smooth cleavage surface, as reflected in the STEM image. Shrinking causes these individual islands to pull toward one another and aggregate into larger clusters of packed chitin sheets held together by strong inter- and intra-chain hydrogen bonds, as seen particularly for P24W and 24W. Gaps between clusters widen as the materials pull away from their original placements, resulting in a cleavage surface that is increasingly rough and grainy. The XRD results indicate crystalline orientations characteristic of chitin being established in the form of larger clusters. The STEM and AFM images support our proposal of material packing with film shrinkage.

3.5. Mechanical properties by uniaxial tensile testing

Figure 7 shows the stress–strain profiles of the chitin films, indicating that the chitin films extend uniformly up to the yield point, followed by strain softening and

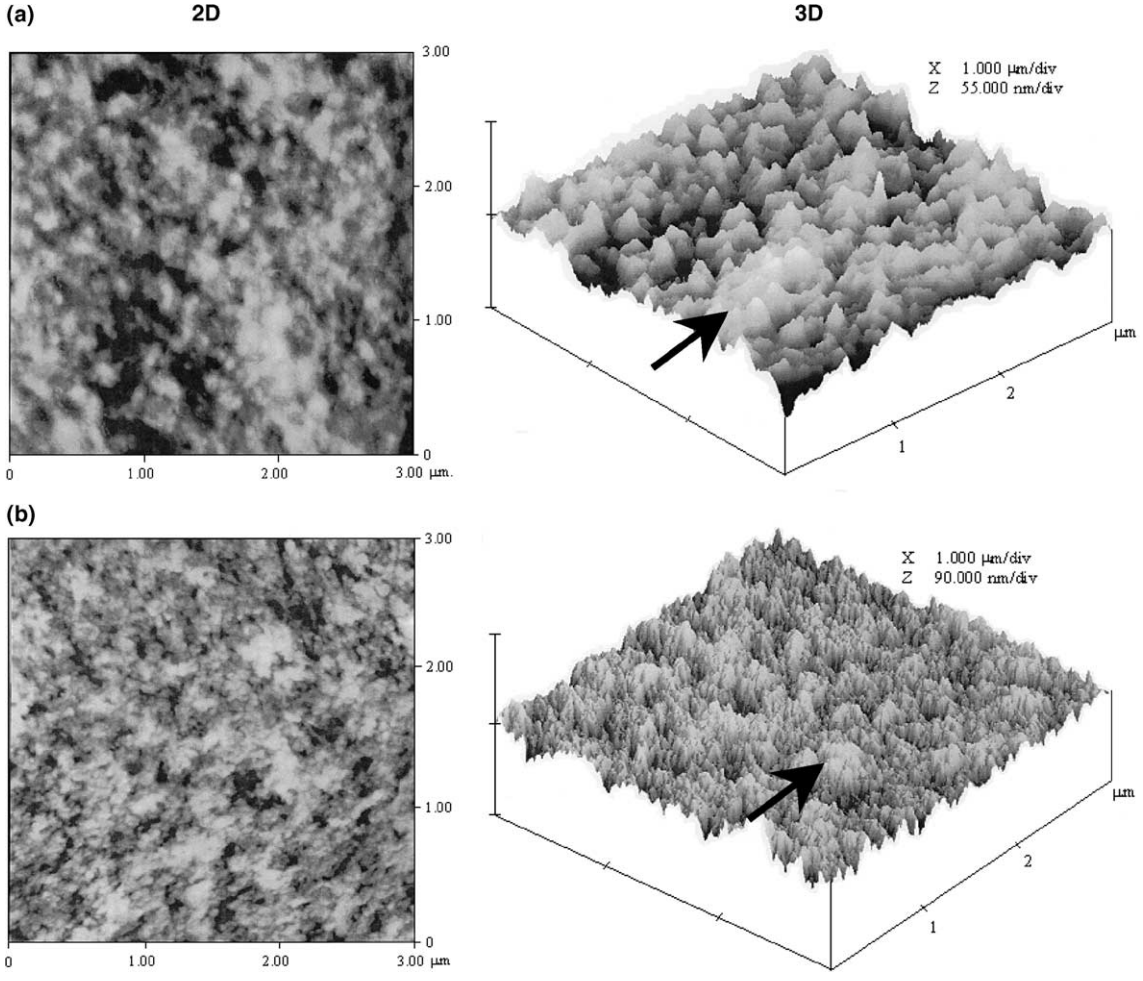

Figure 6. 2D and 3D AFM topography of chitin films: (a) P24, (b) P96, (c) P24W, (d) 24W.

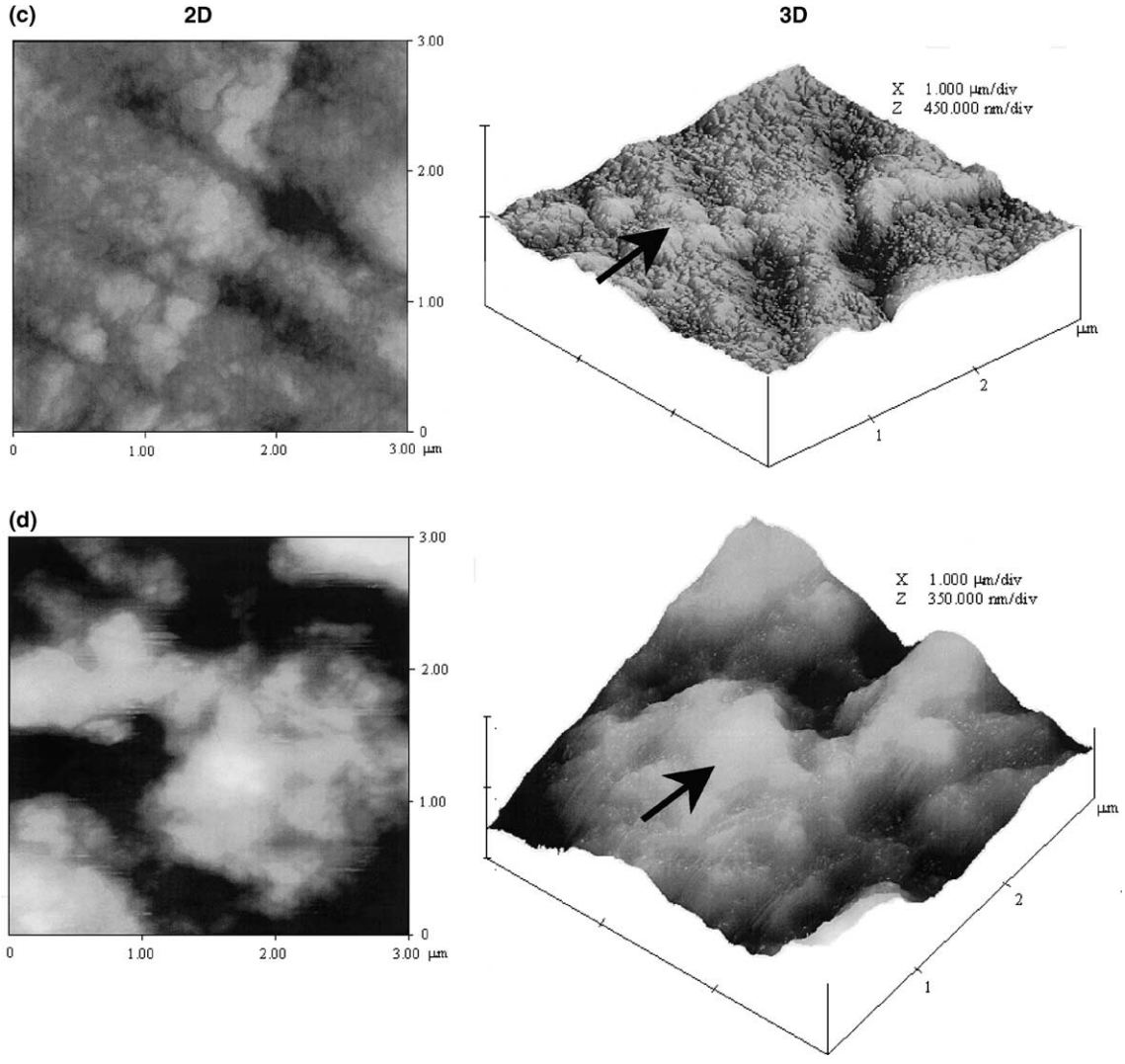

Figure 6 (*continued*)

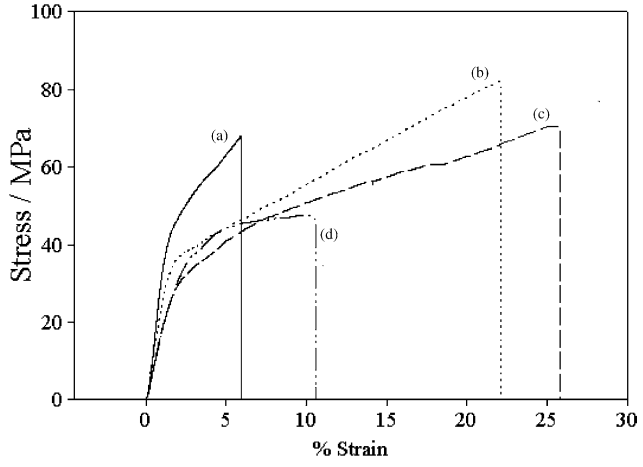

Figure 7. Stress–strain profiles of chitin films: (a) P24, (b) P96, (c) P24W, (d) 24W.

a decrease in the measured stress, until fracture occurs.[22]

Data for tensile and yield strengths, Young's modulus, toughness and maximum percentage strain are found in Table 2. Yield strength was taken as the point where the stress–strain relationship deviated from linearity. There was no significant difference in the tensile strengths and moduli of films P24, P96, and P24W. However, there was a slight progressive decrease in both the yield strength and modulus from films P24, P96, P24W to 24W. When the applied tensile stress exceeded yield strength, films P96 and P24W exhibited substantial plasticity compared to film P24, leading to higher toughness and maximum percentage strains in these two films. Among all the film samples, film 24W had the lowest strength and modulus.

The earlier STEM and AFM discussion focused on the differences in microstructure among the chitin film samples. However, although the characteristic chitin

Table 2. Mechanical properties of chitin films P24, P96, P24W, and 24W

Samples	Tensile strength (MPa)	Yield strength (MPa)	Young's modulus (MPa)	Toughness (MPa)	Maximum strain (%)
P24	60.05 (14.95)	37.83 (3.89)	3659.07 (743.70)	2.05 (1.21)	4.72 (1.79)
P96	77.21 (4.57)	31.06 (2.32)	2703.10 (457.84)	10.53 (1.36)	19.97 (1.68)
P24W	69.63 (5.48)	27.73 (3.10)	2341.21 (312.61)	10.07 (1.52)	21.32 (4.38)
24W	38.34 (9.54)	18.39 (5.90)	1240.74 (469.52)	3.17 (1.30)	9.87 (2.10)

Figures in parentheses = standard deviation.

crystalline orientation became more established toward films P24W and 24W, the positions and shape of the primary peaks remained the same for each film sample, indicating similarity in their overall degree of crystallinity. Chitin is essentially a highly ordered, crystalline structure as evidenced by X-ray diffraction, infrared spectrophotometry, isotope exchange, thermal analysis, hydrolysis, and chromatography.[19,23] In this study, this crystalline order appeared unaffected by the processing method, leading to high tensile strengths for all the chitin film samples, compared to HDPE thin films. Therefore, slight variations in the tensile strengths of films P24, P96, and P24W were attributed to random sampling variability ($P > 0.05$).

The effect of stress on the chitin films is shown on the film surfaces in Figure 8. Slip lines caused by shear yielding are oriented approximately 45° to the tensile axis, and were visible on the surface of plastically deformed film P24W. It appears that two slip systems were operative, as evidenced by two sets of parallel, intersecting lines. Small crack-like entities on film P24W (Fig. 8c) were evidence of crazing. In general, crazing and shear yielding are the two mechanisms responsible for plastic deformation in rigid polymers.[24,25] Slip lines (arrow) were also visible on film P96 (Fig. 8b) but not for film P24 (Fig. 8a). The slip lines on film 24W (Fig. 8d) were generally in the direction of the tensile axis. Therefore, deformation of relatively tougher films P96, P24W, and 24W occurred, possibly when the crystalline sheets formed by shrinkage slid along their slip planes. Film P24 exhibited only slight yielding and fractures at a low percentage strain because slipping was restricted by the sub-microscopic nature of packed chain clusters.

Scanning electron micrographs (SEMs) in Figure 9 show that as shrinkage increased, the top surfaces of the chitin film samples turned from smooth and featureless for film P24 (Fig. 9a) to increasing roughness for films P96 and P24W (Fig. 9b and c). Excessive shrinkage resulted in deep dimples, furrows, and cracks on the top surface of film 24W (Fig. 9d) where smaller chain clusters had pulled away to rearrange into larger clusters, and massive distortion created a fibrous and uneven film surface. Therefore, film 24W had the least strength and modulus values, compared to films P24, P96, and P24W

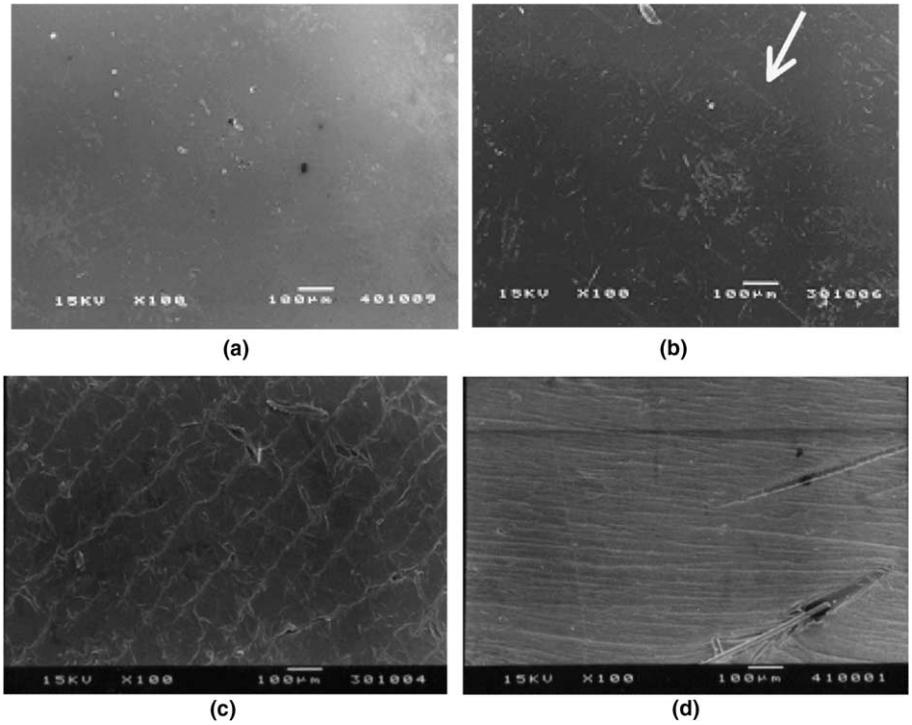

Figure 8. Scanning electron micrographs (SEMs) of the surfaces of stressed chitin films: (a) P24, (b) P96, (c) P24W, (d) 24W.

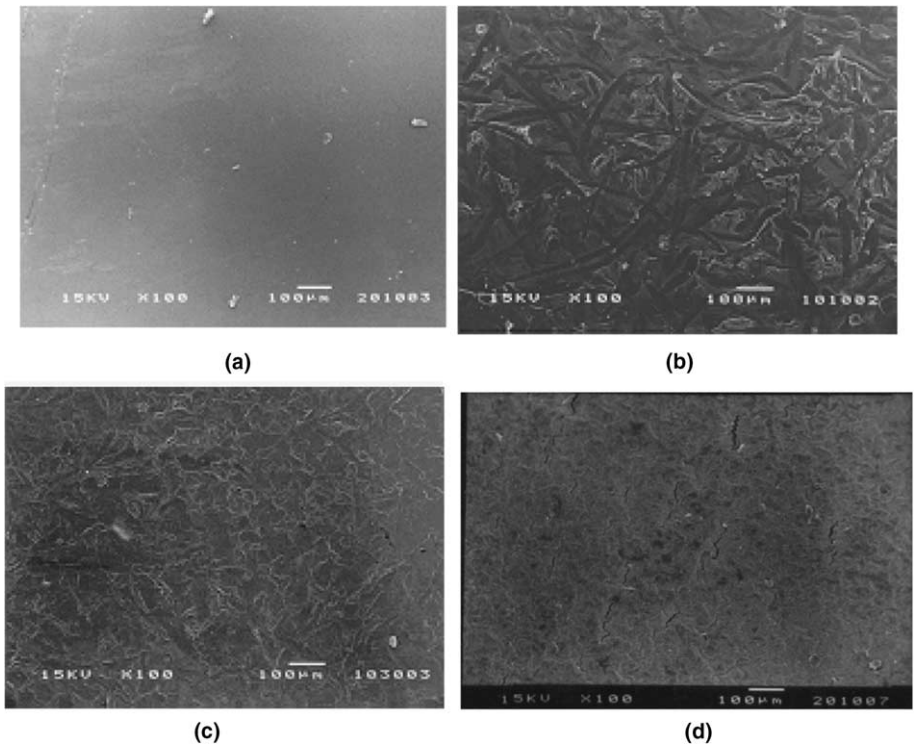

Figure 9. Scanning electron micrographs (SEMs) of the surface of unstressed chitin films: (a) P24, (b) P96, (c) P24W, (d) 24W.

due to these defects. The toughness value of film 24W was close to that of film P24, due to its low strength and decreased ductility.

4. Conclusions

Subjecting chitin gels or films to a mechanical pressure at ambient conditions was referred to herein as cold-press. Cold-press of unwashed chitin gels arrests, to varying degrees, the natural process of shrinking and packing in chitin and used to produce flexible, soft, conformable yet strong chitin films with a texture similar to HDPE thin films. The application of pressure 'immobilizes' chitin chains and 'traps' them into a more loosely consolidated structural morphology impeding the expected formation of extensive inter- and intra-molecular hydrogen bonds.

The process of cold-press permits some flexibility in the manipulation of structure in chitin materials. This has important implications in membrane technology where chitin films have potential use as reverse osmosis membranes. There is an opportunity to tailor chitin films to assume required properties through precise choice and control of processing conditions. Membranes with a range of selectivity may be produced. Such technology can be applied to gas-permeable contact lenses for the eye made from chitin membranes. The flexible chitin films can offer solutions to the biomedical industry in the development of chitin-based wound dressings.

Acknowledgements

This study was supported by a National University of Singapore and National Science and Technology Board grant (R-143-000-014-12). Ms. Nealda L. B. M. Y. is a recipient of a National University of Singapore graduate scholarship.

References

1. Motosugi, K.; Kifune, K. Eur. Pat. Appl. 171254, 1986.
2. Kifune, K.; Hiroyuki, T.; Yamaguchi, Y.; Motosugi, K. Eur. Pat. Appl. 176225, 1986.
3. Yoshikawa, M.; Otsuki, T.; Midorikawa, T.; Terashi T. Eur. Pat. Appl. 794223, 1997.
4. Kifune, K.; Katsuhiro, I.; Shigeru, M. U.S. Patent 4 431 601, 1984.
5. Domard, A.; Grandmontagne, B.; Karibian, T.; Sparacca, G.; Tournebise, H. World Pat. Appl. 97/03708, 1997.
6. Szosland, L. *J. Bioact. Compat. Polym.* **1996**, *1*, 61–71.
7. Shigehiro, H.; Usutani, A. *Int. J. Biol. Macromol.* **1997**, *20*, 245–249.
8. Gorovoj, L.; Burdukova, L. *Adv. Chitin Sci.* **1996**, *1*, 430–439.

9. Ohshima, Y.; Nishino, K.; Yonekura, Y.; Kishimoto, S.; Wakabayashi, S. *Eur. J. Plast. Surg.* **1987**, *10*, 66–69.
10. Sagar, B.; Hamlyn, P.; Wales, D. Brit. Patent 2 165865, 1986.
11. Sagar, B.; Hamlyn, P.; Wales, D. Eur. Pat. Appl. 460774, 1991.
12. Kifune, K.; Yamaguchi, Y.; Tanze, H. Eur. Pat. Appl. 199531, 1986.
13. Uragami, T.; Ohsumi, Y.; Sugihara, M. *Polymer* **1981**, *22*, 1155–1156.
14. Rutherford, F. A.; Dunson, W. A. In *Chitin Chitosan and Related Enzymes*; Zikakis, J. P., Ed.; Academic: New York, 1984; pp 135–143.
15. Callister, W. D., Jr. In *Materials Science and Engineering: An Introduction*, 4th ed.; Wiley: New York, 1997; pp 426–429.
16. Seong, S. K.; Seon, J. K.; Yoon, D. M.; Young, M. L. *Polymer* **1994**, *35*, 3212–3216.
17. Seong, S. K.; Su, H. K.; Young, M. L. *J. Polym. Sci. B: Polym. Phys.* **1996**, *34*, 2367–2374.
18. Takai, M.; Shimizu, Y.; Hayashi, J.; Tokura, S.; Ogawa, M.; Kohriyama, T.; Satake, M.; Fujita, T. *ACS Symp. Ser.* **1992**, *489*, 38–52.
19. Muzzarelli, R. A. A. *Natural Chelating Polymers*; Pergamon: New York, 1973; p 113.
20. Muzzarelli, R. A. A. *Natural Chelating Polymers*; Pergamon: New York, 1973; p 134.
21. Austin, P. R.; Brine, C. J. U.S. Patent 4 029 727, 1977.
22. Ward, I. M. *Mechanical Properties of Solid Polymers*; Wiley-Interscience: London, 1971; p 274.
23. Roberts, G. A. F. *Chitin Chemistry*; Macmillan: London, 1992; p 21.
24. Callister, W. D., Jr. In *Materials Science and Engineering: An Introduction*, 4th ed.; Wiley: New York, 1997; pp 156–158.
25. Young, R. J. Polymer Strength. In *Comprehensive Polymer Science. The Synthesis, Characterization, Reactions and Applications of Polymers*; Booth, C., Price, C., Eds.; Pergamon: Oxford, 1989; pp 511–532.